ELSEVIER

Chemical Engineering Journal 143 (2008) 32–42

Chemical Engineering Journal

www.elsevier.com/locate/cej

Equilibrium and kinetic data, and adsorption mechanism for adsorption of lead onto valonia tannin resin

Mahmut Özacar[a,*], İ. Ayhan Şengil[b], Harun Türkmenler[c]

[a] *Department of Chemistry, Science & Arts Faculty, Sakarya University, 54140 Sakarya, Turkey*
[b] *Department of Environmental Engineering, Engineering Faculty, Sakarya University, 54040 Sakarya, Turkey*
[c] *Institute of Sciences and Technology, Sakarya University, 54040 Sakarya, Turkey*

Received 2 September 2006; received in revised form 28 December 2006; accepted 9 December 2007

Abstract

The adsorption of lead onto valonia tannin resin studied using a batch adsorber. The aim of this study was to understand the mechanisms that govern lead removal and find a suitable equilibrium isotherm and kinetic model for the lead removal in a batch reactor. The experimental isotherm data were analyzed using the Langmuir, Freundlich, Temkin and Dubinin–Radushkevich equations. The equilibrium data fit well the Langmuir isotherm. The experimental data were analyzed using four adsorption kinetic models – the pseudo first- and second-order equations, the Elovich equation and intraparticle diffusion equation – to determine the best fit equation for the adsorption of lead-ions onto valonia tannin resin. The characteristic parameters for each kinetic models have been determined and the correlation coefficients have been calculated in order to assess which model provides the best fit predicted data with experimental results. Also, predicted q_t values from the kinetic equations were compared with the experimental data. Results show that the pseudo second-order equation provides the best correlation for the adsorption process. Adsorption mechanism was also proposed for the adsorption of lead-ions onto valonia tannin resin.

Keywords: Valonia tannin resin; Lead; Adsorption kinetics and isotherms; Pseudo second-order equation; Adsorption mechanism; FTIR studies

1. Introduction

Industrialization in many regions has increased the discharge of industrial wastes, especially those containing heavy metals, into water bodies or on land. The presence of heavy metals in the aquatic ecosystem poses human health risks and causes harmful effects to living organisms in water and also to the consumers of them. The wastewater from mining, painting and printing processes, plumbing, automobile battery and petrochemical industries contains undesired amounts of Pb(II) ions. In industrial wastewaters, lead-ion concentrations approach 200–500 mg/L; this concentration is very high in relation to water quality standards, and lead-ion concentration of wastewaters must be reduced to a level of 0.05–0.10 mg/L before discharge to water ways or sewage systems [1,2].

Many methods have been used to remove the heavy metals from wastewaters, namely, coagulation, precipitation, flotation, solvent extraction, membrane filtration, reverse osmosis, ion exchange, adsorption, etc. have been reported in the literature, but few of them were accepted due to cost, low efficiency, disposal of sludge, inapplicability to a wide range of pollutants. The adsorption process is one of the effective methods used to remove heavy metals from aqueous solution. Activated carbon has long been used as a highly efficient adsorbent for the removal of numerous heavy metals from water [3]. However, it is an expensive material but regeneration is relatively easy, but this adds to the operational costs. Up to now, numerous experimental studies on Pb^{2+} adsorption by clays [4], activated phosphate [5], chitosan nanoparticles [6], peat or peat resin [7,8], sawdust [9], condensed tannin resin [10,11], etc. have been published.

Tannins have multiple adjacent phenolic hydroxyls and exhibit specific affinity to metal ions. Thus they can be used as an alternative and effective adsorbent for the removal and recovery of metal ions from water. However, tannins are water-soluble compounds, thus when they are used directly as an adsorbent for recovery of metal from aqueous systems, they have the disadvantage of being dissolved by water. To overcome this drawback, various immobilization attempts tired have cited

* Corresponding author. Fax: +90 264 2955950.
E-mail address: mozacar@hotmail.com (M. Özacar).

1385-8947/$ – see front matter © 2007 Elsevier B.V. All rights reserved.
doi:10.1016/j.cej.2007.12.005

in elsewhere [12]. The gallic acid units of gallotannin are reactive with formaldehyde due to the strong nucleophilicity of their ring, and are available to complex or ion exchange with metal ions because of the hydroxyls groups present in their rings. In the literature, some researchers synthesized sorbents from commercial condensed tannin extracts and applied them in removal of heavy metals such as uranium, americium, copper, chromium, cadmium, vanadium and lead [11,13–17]. These examinations include determination of sorbent capacity, influence of operating parameters and, some of them, presumption of binding mechanisms. Condensed tannins were also used as adsorbent starting materials in all of these studies. But the studies of sorption kinetics in the removal of metal ions from effluents using tannin-based sorbent have not been reported.

This paper primarily focused on the adsorption kinetics of valonia tannin resin (VTR, hydrosable tannin). The batch agitation studies were performed to investigate the influence of initial lead concentration on the adsorption rate. Four kinetic models including pseudo first- and second-order equations, the Elovich equation and Intraparticle diffusion equation were used to describe the adsorption process. The adsorption isotherm was measured in order to evaluate the discrepancy between the experimental data and the theoretical equilibrium capacity predicted from the kinetic equations. These fundamental data will be useful for further applications in the treatment of practical waste or process effluents.

2. Materials and methods

2.1. Materials

The commercial valonia tannin (VT) extract was obtained from Tuzla Dericiler Sanayi Sitesi, İstanbul-Türkiye. The tannin content of the extract was determined to be 70% as gallotannin according to the Prussian Blue-test [18] and the Rhodanine-test [19]. The extract which is considered its tannin content was used in the polymerization experiments without further purification. All other chemicals used in the studies were analytical grade and obtained from Merck Chemical Co.

2.2. Preparation of valonia tannin resin (VTR)

11.45 g of commercial valonia extract powder corresponding to a hydrolysable tannin powder (8 g or 6.80×10^{-3} mol of gallotannin) was added to 50 mL of 13.3N (0.665 mol) aqueous ammonia, followed by stirring for 5 min to dissolve it. To the resulting solution was added 65 mL of an aqueous solution containing 37% formaldehyde (0.874 mol), followed by stirring for 5 min for uniform mixing. When this stirring was stopped, a yellow precipitate formed. After the resulting liquid containing the precipitate was stirred for 30 min, and then the formed suspension was filtered through filter paper. The precipitate thus obtained was added to 50 mL distilled water, and heated at 343 K for 3 h with stirring to remove free formaldehyde. The heated suspension was filtered. Subsequently, the precipitate thus obtained was added to 100 mL of 0.1N HNO_3, followed by stirring for 30 min. The liquid containing the precipitate is mixed with mineral acid such as nitric, hydrochloric and sulfuric acid to make the precipitate insoluble in acidic and basic medium. Finally, the HNO_3 solution was filtered and washed with distilled water, followed by drying the filtered precipitate at 353 K to thereby obtain an insoluble tannin resin. The valonia tannin (hydrolysable tannin) resin (VTR) was sieved to give different particle size fractions using ASTM standard sieves, and 75–100 μm particle size was used in the adsorption experiments. The BET specific surface area was measured to be 11.70 m^2/g from N_2 adsorption isotherms with a sorptiometer (Micromeritics FlowSorb II-2300).

2.3. Adsorption studies

The lead solutions were prepared by dissolving the $Pb(NO_3)_2$ in appropriate amounts in distilled water. In the determination of equilibrium adsorption isotherm, 0.1 g VTR and 100 mL of the chosen desired concentration of $Pb(NO_3)_2$ solutions were transferred in 250 mL flask, and shaken on a horizontal bench shaker (Nüve SL 250), operating at 200 rpm, for 180 min (the time required for equilibrium to be reached between Pb^{2+} adsorbed and Pb^{2+} in solution) using a bath to control the temperature at 298 ± 2 K. The experiments were performed at the initial pH 4 of lead solution which was found to be optimum pH in previous studies (results not shown). The pH of the solutions was adjusted with HCl or NaOH solution by using a pH meter. At the end of the adsorption period, the samples (5 mL) were taken and centrifuged for 15 min at 5000 rpm and then analyzed using AAS equipped with an auto-sampler (Shimadzu AA6701F). The amount of adsorption at equilibrium, q_e (mmol/g), was computed as follows:

$$q_e = \frac{(C_0 - C_e)V}{W} \quad (1)$$

where C_0 and C_e are the initial and equilibrium solution concentrations (mmol/L), respectively, V the volume of the solution (L) and W is the weight of VTR used (g).

In the experiments of batch kinetic adsorption, 2 L of the chosen desired concentration of $Pb(NO_3)_2$ solutions were placed in jar-test apparatus together with 2 g VTR and mixed at 150 rpm. At predecided intervals of time, samples were taken, and their concentrations were determined.

2.4. FTIR Studies

FTIR spectra were recorded on a Mattson Intensity Series FTIR spectrophotometer. The samples were prepared after removing the supernatant, and a portion of the residue was filtered through 0.45 μm Millipore membrane filters. The remaining portion was dried at 353 K for 4 h. Potassium bromide disks were prepared by mixing 1 mg of these samples with 200 mg of KBr (spectrometry grade) at 10,000 kg/cm^2 pressure for 30 min under vacuum. The spectra were recorded from 4000 to 400 cm^{-1} (100 scans) on samples in KBr disks.

3. Results and discussion

3.1. Equilibrium studies

The successful representation of the dynamic adsorptive separation of solute from solution onto an adsorbent depends upon a good description of the equilibrium separation between the two phases. By plotting solid phase concentration against liquid phase concentration graphically it is possible to depict the equilibrium adsorption isotherm. Fig. 1 shows the equilibrium adsorption of lead (q_e versus C_e) using VTR. The plot of lead uptake against equilibrium concentration indicates that adsorption increases initially with concentration but then reaches saturation. The decrease in the curvature of the isotherm, at it tends to a monolayer, as the C_e values increase considerably for a small increase in q_e, is possibly due to the less active sites being available at the end of the adsorption process and/or the difficulty of the edge solutes in penetrating the adsorbent, lead-ions partially covering the surface sites of VTR.

Adsorption isotherms are important for the description of how molecules or ions of adsorbate interact with adsorbent surface sites and also, are critical in optimizing the use of adsorbent. Hence, the correlation of equilibrium data using either a theoretical or empirical equation is essential for the adsorption interpretation and prediction of the extent of adsorption. Four isotherm equations have been tested in the present study, namely, Langmuir, Freundlich, Temkin and Dubinin–Radushkevich.

The Langmuir adsorption isotherm is based on the assumption that all adsorption sites are equivalent and adsorption in an active sites is independent of whether the adjacent sites is occupied or not. The data of the uptake of lead has been processed in accordance with the Langmuir isotherm equation [20–22]:

$$q_e = \frac{K_L C_e}{1 + a_L C_e} \tag{2}$$

A linear form of this expression is:

$$\frac{C_e}{q_e} = \frac{1}{K_L} + \frac{a_L}{K_L} C_e \tag{3}$$

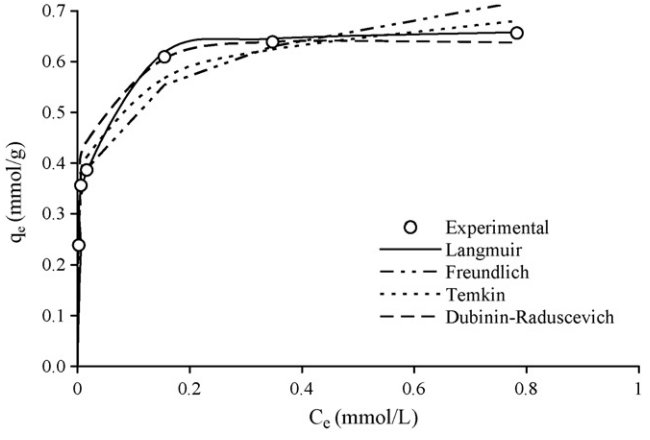

Fig. 1. Equilibrium isotherms of lead on VTR. Conditions: 75–100 μm particle size, 0.1 g/100 mL dose, 298 K temperature and pH 4.

where q_e (mmol/g) and C_e (mmol/L) are the amount of adsorbed lead per unit weight of adsorbent and unadsorbed lead concentration in solution at equilibrium, respectively. The constant K_L is the Langmuir equilibrium constant and the K_L/a_L gives the theoretical monolayer saturation capacity, Q_0. Therefore, a plot of C_e/q_e versus C_e gives a straight line of slope a_L/K_L and intercepts $1/K_L$.

The values of the Langmuir constants a_L, K_L and Q_0 with the correlation coefficient are listed in Table 1 for the lead–VTR system and the theoretical Langmuir isotherm is plotted in Fig. 1 together with the experimental data points. The value of the correlation coefficient is higher than the other three isotherms values. In all cases, the Langmuir equation represents the best fit of experimental data than the other isotherm equation (Fig. 1). The monolayer saturation capacity, Q_0, is 0.668 mmol/g. The lead adsorption capacities of some adsorbents are given in Table 2. It is seen from Table 2 that the capacity of VTR is better than most of the adsorbents reported in the literature.

The other isotherms [20,22–26] tested in the present study are represented by Eqs. (4)–(6):

- Freundlich isotherm:

$$q_e = K_F C_e^{1/n} \tag{4}$$

Temkin isotherm:

$$q_e = \frac{RT}{b} \ln (A C_e) \tag{5}$$

Dubinin–Radushkevich isotherm:

$$q_e = q_m e^{-\beta \varepsilon^2} \tag{6}$$

The linear form of the Freundlich, Temkin and Dubinin–Radushkevich isotherms can be expressed by

Table 1
Langmuir, Freundlich, Temkin and Dubinin–Radushkevich isotherm constants

Langmuir	
K_L (L/g)	53.19
a_L (L/mmol)	79.53
Q_0(mmol/g)	0.668
r^2	0.999
Freundlich	
K_F (L/g)	0.746
n	6.266
r^2	0.900
Temkin	
B	0.070
A (L/g)	21,406
r^2	0.965
Dubinin–Radushkevich	
q_m (mmol/g)	0.669
β (mmol^2/J^2)	4×10^{-9}
r^2	0.976

Conditions: 75–100 μm particle size, 0.1 g/100 mL dose, 298 K temperature and pH 4.

Table 2
Monolayer adsorption capacities (Q_0 in mg/g) in the literature for adsorption of Pb^{2+} on various adsorbents

Adsorbent	Q_0 (mg/g)	Reference
Chitosan nanoparticles	398	[6]
Condansed tannin gel	190	[59]
Activated phosphate	155	[5]
Valonia tannin resin	138.3 (0.668 mmol/g)	This study
Chitosan	115.5 (0.558 mmol/g)	[60]
Natural phosphate	115	[5]
Condansed tannin resin	114.9	[11]
Modified rice husk	108	[61]
Peat	103.1	[62]
Zeolite	70.58	[63]
PHEMA/chitosan membranes	68.81	[64]
Gelidium algae	64	[1]
Ethanol-treated yeast biomass	60.24	[65]
Activated carbon (Sorbo-Norit)	54.10	[66]
Bacteria modified activated carbon (Sorbo-Norit)	54.10	[66]
Modified peat-resin particles	47.39	[7]
Algal waste	44	[1]
Live biomass	35.69	[67]
Bacteria modified activated carbon (Merck)	26.40	[66]
Humic acid	22.70	[68]
Activated carbon (Merck)	21.50	[66]
Coir	19.87 (0.096 mmol/g)	[21]
Carbon nanotubes	17.44	[69]
Jute	17.18 (0.083 mmol/g)	[21]
Sawdust	12.63 (0.061 mmol/g)	[21]
Groundnut shells	12.21 (0.059 mmol/g)	[21]
Goethite	11.04	[68]
Montmorillonite	10.40	[68]
Sawdust	3.19	[9]
Waste tea leaves	2.096	[70]

Eqs. (7)–(9), respectively:

$$\log q_e = \log K_F + \frac{1}{n}\log C_e \quad (7)$$

$$q_e = B \ln A + B \ln C_e \quad (8)$$

$$\ln q_e = \ln q_m - \beta\varepsilon^2 \quad (9)$$

where $B = RT/b$, K_F is the Freundlich constant, n the Freundlich exponent, A and B are the Temkin constants, q_m the Dubinin–Radushkevich monolayer capacity (mmol/g), β a constant related to adsorption energy, and ε is the Polanyi potential which is related to the equilibrium concentration as follows:

$$\varepsilon = RT \ln\left(1 + \frac{1}{C_e}\right) \quad (10)$$

where R is the gas constant (8.31 J/mol K) and T is the absolute temperature. The constant β gives the mean free energy, E, of sorption per molecule of the sorbate when it is transferred to the surface of the solid from infinity in the solution and can be computed using the relationship [25,26]:

$$E = \frac{1}{\sqrt{2\beta}} \quad (11)$$

K_F and n can be determined from the linear plot of $\log q_e$ versus $\log C_e$. The values of the Freundlich constants together with the correlation coefficient are presented in Table 1 and the theoretical Freundlich equation is shown in Fig. 1. The value of correlation coefficient is much lower than the other three isotherm values. In all cases, the Freundlich equation represents the poorest fit of experimental data than the other isotherm equation (Fig. 1).

The adsorption data can also be analyzed according to Eq. (7). Therefore a plot of q_e versus $\ln C_e$ enables one to determine the constants A and B. The values of the Temkin constants A and B are listed in Table 1 and the theoretical plot of this isotherm is shown in Fig. 1. The correlation coefficient is also listed in Table 1 and is higher than the Freundlich value but lower than Langmuir and Dubinin–Radushkevich value. Therefore, the Temkin equation only represents a better fit of experimental data than the Freundlich equation but not in the cases of both Langmuir and Dubinin–Radushkevich equations (Fig. 1).

The Dubinin–Radushkevich constants are calculated and given in Table 1 and the theoretical Dubinin–Radushkevich isotherm is plotted in Fig. 1 together with the experimental data points. Also, the correlation coefficient has been determined and is shown in Table 1 and the value of correlation coefficient is higher than both Freundlich and Temkin values but lower than Langmuir value. Therefore, the Dubinin–Radushkevich equation represents a better fit of experimental data than both Freundlich and Temkin equations but not in the case of Langmuir equation (Fig. 1).

As seen from Table 1 and Fig. 1, the Langmuir isotherm shows a better fit to adsorption data than the other isotherm equations. The fact that the Langmuir isotherm fits the experimental data very well may be due to homogenous distribution of active sites on the VTR surface; since the Langmuir equation assumes that the surface is homogenous [20]. This situation may be explained based on the structure of VTR, containing of same surface reactive –OH groups such as pyrogallol groups binding lead-ions.

3.2. Kinetic studies

Effects of contact time and initial lead concentration on adsorption of Pb^{2+} by VTR are shown in Fig. 2. The amount of Pb^{2+} adsorbed increased with increase in contact time and reached equilibrium after 90 min. The equilibrium time is independent of initial lead concentration. But in the first 30 min, the initial rate of adsorption was greater for higher initial lead concentration. Because the diffusion of lead-ions through the solution to the surface of adsorbent is affected by the lead concentration, since mixing speed is constant. An increase of lead concentration accelerates the diffusion of Pb^{2+} from the solution onto adsorbent due to the increase in the driving force of the concentration gradients [20].

The mechanism of adsorption often involves chemical reaction between functional groups present on the adsorbent surface and the metal ions or hydrolysed species. This involves, inmost cases, formation of metal organic complexes or cation exchange reactions because of high cation exchange capacity of the

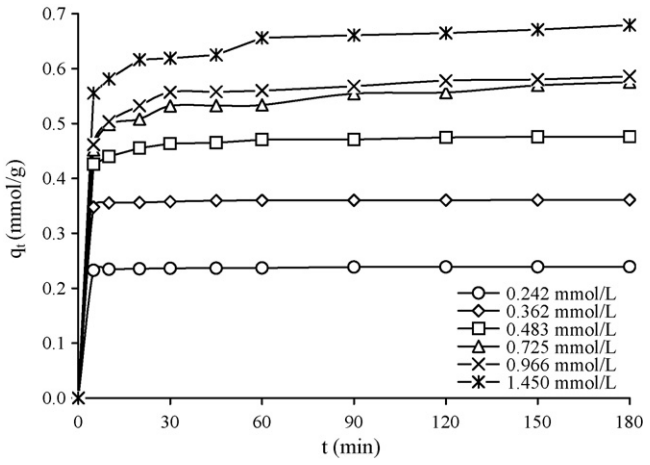

Fig. 2. Adsorption kinetics of lead on VTR at different initial lead concentration. Conditions: 75–100 μm particle size, 2 g/L dose, 298 K temperature and pH 4.

adsorbents. Other possible mechanisms involve mass-transport processes, bulk transport in the liquid phase, diffusion across the liquid film surrounding the adsorbent particles, and diffusion into micropores and macropores. The important characteristics of the adsorbent that determine equilibrium capacity and rate are the surface area, the physicochemical nature of the surface, the availability of that surface to adsorbate molecules or ions, the physical size and from of the adsorbent particles. System parameters such as pH, temperature and mixing speed can also markedly influence the adsorption as they affect one or more of above parameters [27–29].

Up to now, several kinetic models such as the pseudo first- and second-order equations, the Elovich equation and intraparticle diffusion equation are used to examine the controlling mechanism of adsorption process, such as chemical reaction, diffusion control and mass transfer. Those models have been applied in certain specific cases [23,27,30–32].

The linear pseudo first-order equation is given as follows:

$$\log(q_e - q_t) = \log q_e - \frac{k_1}{2.303}t \tag{12}$$

where q_t and q_e are the amounts of lead adsorbed at time t and at equilibrium (mmol/g), respectively, and k_1 is the rate constant of pseudo first-order adsorption process (1/min). The slopes and intercepts of plots of $\log(q_e - q_t)$ versus t were used to determine the first-order rate constant k_1 and equilibrium adsorption density q_e. A comparison of the results with the correlation coefficients is shown in Table 3. The correlation coefficients for the first-order kinetic model obtained at all the studied concentrations were low. It was also observed in the present work that q_e values computed from the Lagergren plots deviated considerably from the experimental q_e values. This indicates that pseudo first-order equation might not be sufficient to describe the mechanism of Pb^{2+}–VTR interactions [27].

The pseudo second-order equation [27,30–34], given by

$$\frac{dq_t}{dt} = k_2(q_e - q_t)^2 \tag{13}$$

Table 3
Comparison of the pseudo first- and second-order equations, the Elovich equation and intraparticle diffusion equation rate constants, and calculated and experimental q_e values for different initial lead concentrations

C_0 (mmol/L)	$q_{e,exp.}$ (mmol/g)	Pseudo first-order equation			Pseudo second-order equation			Intraparticle diffusion		Elovich equation		
		k_1 (1/min)	$q_{e,cal.}$ (mmol/g)	r^2	k_2 (g/mmol min)	$q_{e,cal.}$ (mmol/g)	r^2	k_p (mmol/g min$^{1/2}$)	r^2	α (mmol/g min)	β (g/mmol)	r^2
0.242	0.239	2.56×10^{-2}	0.007	0.977	11.09	0.240	1	0.70×10^{-3}	0.876	5.66×10^{52}	555.6	0.977
0.362	0.361	2.07×10^{-2}	0.007	0.866	11.14	0.361	1	1.90×10^{-3}	0.796	9.58×10^{45}	322.6	0.844
0.483	0.476	3.41×10^{-2}	0.051	0.932	2.142	0.478	1	7.80×10^{-3}	0.910	1.76×10^{11}	73.53	0.935
0.725	0.575	1.73×10^{-2}	0.100	0.931	0.594	0.578	0.999	13.5×10^{-3}	0.796	2.46×10^{4}	32.68	0.957
0.966	0.586	1.89×10^{-2}	0.085	0.921	0.782	0.589	0.999	17.3×10^{-3}	0.840	2.52×10^{4}	31.65	0.926
1.450	0.679	1.77×10^{-2}	0.105	0.946	0.582	0.683	0.999	16.3×10^{-3}	0.923	9.48×10^{4}	29.41	0.974

Conditions: 75–100 μm particle size, 2 g/L dose, 298 K temperature and pH 4.

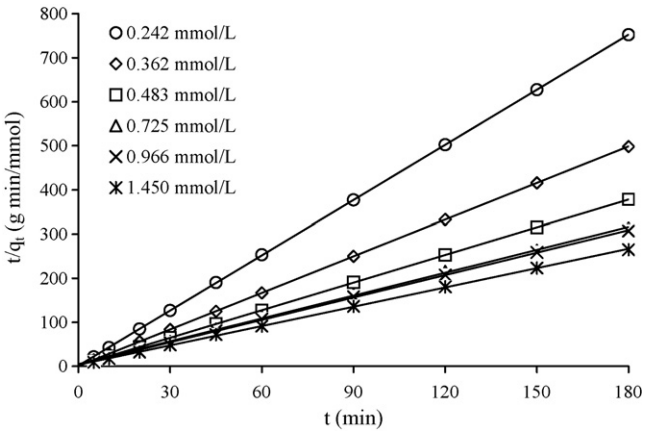

Fig. 3. Plot of the pseudo second-order equation for the adsorption kinetics of lead on VTR at different initial concentration.

where k_2 is the pseudo second-order rate constant (g/mmol min) is applicable. For the boundary conditions $t = 0$ to $t = t$ and $q_t = 0$ to $q_t = q_t$, the integrated form of equation is

$$\frac{1}{(q_e - q_t)} = \frac{1}{q_e} + k_2 t \tag{14}$$

which can also be rearranged to obtain a linear form:

$$\frac{t}{q_t} = \frac{1}{k_2 q_e^2} + \frac{1}{q_e} t \tag{15}$$

If the pseudo second-order equation is applicable, the plot of t/q_t versus t gives a linear relationship, which allows computation of k_2 and q_e without having to know any parameter beforehand. The pseudo second-order model based on the Eq. (15), which considers the rate-limiting step as the formation of chemisorptive bond involving sharing or exchange of electrons between adsorbate and the adsorbent, was therefore applied. The plot of t/q_t versus t (Fig. 3) yields very good straight lines for different initial lead concentrations. Table 3 lists the computed results obtained from the second-order equation. The correlation coefficients for the second-order kinetic equation were greater than 0.999 for all concentrations. The calculated q_e values also agree very well with the experimental data. These indicate that the adsorption system studied belongs to the second order kinetic model.

The adsorption data may also be analyzed using the Elovich equation [27,31,35,36], which has the linear form:

$$q_t = \frac{1}{\beta} \ln(\alpha\beta) + \frac{1}{\beta} \ln t \tag{16}$$

where α is the initial sorption rate constant (mmol/g min), and the parameter β is related to the extent of surface coverage and activation energy for chemisorption (g/mmol).

The constants can be obtained from the slope and intercept of the plot of q_t versus $\ln t$. In this case, a linear relationship was obtained between Pb^{2+} adsorbed, q_t, and $\ln t$ over the whole adsorption period, with correlation coefficients between 0.844 and 0.977 for all the lines (Table 3). Also Table 3 lists the kinetic constants obtained from the Elovich equation. In the case of using the Elovich equation, the correlation coefficients are lower than those of the pseudo second-order equation. The Elovich equation does not predict any definite mechanism, but it is useful in describing adsorption on highly heterogeneous adsorbents [27]. This situation indicates that the Elovich equation might not be sufficient to describe the mechanism, since VTR possesses highly homogenous surface active sites such as pyrogallol groups.

The variation in the amount of adsorption with time at different initial metal ion concentrations can be used to evaluate the role of diffusion in the adsorption process. The intraparticle diffusion rate constant (k_p) is given by the equation [23,27,32]:

$$q_t = k_p t^{1/2} \tag{17}$$

where k_p is the intraparticle diffusion rate constant (mmol/g min$^{1/2}$). Such plots may present a multilinearity [23,32], indicating that two or more steps take place. The first, sharper portion is attributed to the diffusion of adsorbate through the solution to the external surface of adsorbent or the boundary layer diffusion of solute molecules or ions. The second portion describes the gradual adsorption stage, where intraparticle diffusion is rate limiting. The third portion is attributed to the final equilibrium stage where intraparticle diffusion starts to slow down due to extremely low adsorbate concentrations in the solution. The rate of uptake might be limited by size of adsorbate molecule or ion, concentration of the adsorbate and its affinity to the adsorbent, diffusion coefficient of the adsorbate in the bulk phase, the pore size distribution of the adsorbent, and degree of mixing [37].

Fig. 4 shows a plot of the linearized form of the intraparticle diffusion model at all concentrations studied. It can be seen that the plots are not linear over the whole time range, implying that more than one process affects the lead adsorption. The multiple nature of these plots can be explained by boundary layer diffusion which gives the first portion and the intraparticle diffusion that gives further two linear portion. If the intraparticle diffusion is the only rate-controlling step the plot passes through the origin; if not, the boundary layer diffusion controls the adsorption to some degree and this further that the intraparticle diffusion is not the only rate controlling step, but also other processes may control the rate of adsorption [37,38]. It can be deduced from

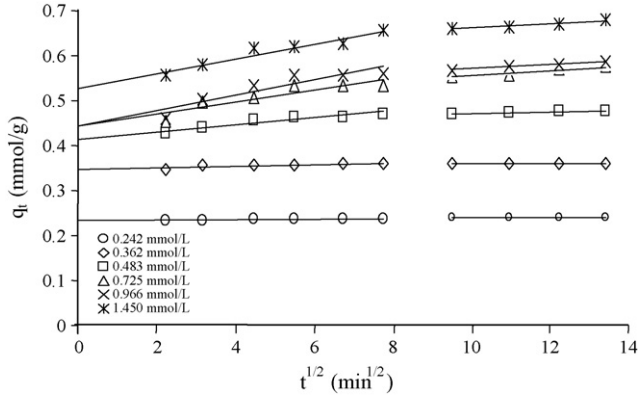

Fig. 4. Plot of the intraparticle diffusion equation for the adsorption of lead on VTR at different initial concentration.

multi-linear plots that are more than one process that control the rate of adsorption but only one is rate limiting. The slope of the linear portion indicates the rate of adsorption. The lower slope corresponds to a slower adsorption process. As shown in Fig. 4, the external surface adsorption (stage 1) is absent. Stage 1 is completed before 5 min., and then the stage of intraparticle diffusion control (stage 2) is attained and continues from 5 to 60 min. Finally, final equilibrium adsorption (stage 3) starts after 60 min. The lead-ions are slowly transported *via* intraparticle diffusion into the particles and are finally retained in the micropores. The slope of the second linear portion characterizes the rate parameter corresponding to the intraparticle diffusion, whereas the intercept of this second portion is proportional to the boundary layer thickness. The rate parameters, k_p, together with the correlation coefficients are also listed in Table 3.

The pseudo second-order kinetic model provides the best correlation for all of the adsorption process whereas the pseudo first-order, the Elovich and intraparticle diffusion equations do not give a good fit to the experimental data for the adsorption of lead. This suggest that the lead-VTR adsorption system belongs to the second-order equation, based on the assumption that the rate limiting step may be chemical sorption or chemisorption involving valency forces through sharing or exchange of electrons between VTR and lead.

3.3. Adsorption mechanism

The Langmuir isotherm and pseudo second-order kinetic model provide best correlation with the experimental data for the adsorption of lead-ions onto VTR for different initial lead concentrations over the whole range studied. Both Langmuir isotherm and pseudo second-order kinetic model assume that the VTR surface, containing the same reactive –OH groups such as pyrogallol groups binding lead-ions, is homogenous and the operating adsorption mechanism is chemisorption involving valency forces through sharing or exchange of electrons between lead and VTR. The homogenous surface of VTR provides multisites to the lead-ions. Therefore, the pseudo second-order equation, which was used in various molecules or ions chemisorption onto homogenous surface, can be fitted to the adsorption of lead-ions very well.

In the literature, different adsorption mechanism for the adsorption of metals onto tannin-based adsorbents have been proposed. The mechanism by which metal ions are adsorbed onto different tannin resins has been a matter of considerable debate. Different studies have reached different conclusions. These include ion-exchange, surface adsorption, chemisorption, complexation, and adsorption–complexation [10,11,39–43]. It is commonly believed that ion-exchange is most prevalent mechanism. Metals react with phenolic groups of the tannin resins to release protons with their anion sites to displace an existing metal. Based on the complex polyhydric phenolic nature of the VTR, a possible mechanism of ion exchange could be considered as Pb^{2+} attaching itself to adjacent hydroxyl groups and oxyl groups which could donate two pairs of electrons to lead-ions, forming chelated compounds and releasing two hydrogen ions into solution [39,44].

Other studies have found evidence that tannin resins take up metals by complexation, surface adsorption, and chemisorption [39,41,43,45]. The hydroxyl groups in tannins offer special opportunities for formation of metal complexes. Lead forms complexes with the phenolics with two adjacent hydroxyls (catechols), and the presence of a third adjacent hydroxyl (pyrogallols) increases the stability of the complexes [40,43]. The chemisorptive bond could be formed by sharing a pair of electrons, from the organic adsorbent, with metals. The organic adsorbent, containing O, N, P, or S, are usually regarded as the reaction centre for the chemisorption process. Natural tannin derivatives are oxygen-containing adsorbents; therefore, formation of lead–oxygen bond is possible [39,43].

Several studies support the general view that the reaction of metal ions, such as Cu, Fe and Pb with tannin resin is one of chelate ring formation involving adjacent aromatic carboxylate –COOH and phenolic –OH groups or, less commonly, two adjacent –COOH groups which participate in ion-exchange reactions by binding metal ions with release of H^+ ions [10,13,39,41–44].

Surface adsorption is another mechanism by which metal ions may be bound to tannin resin. This mechanism is a surface reaction where a positively charged metal ion is attracted to a negatively charged surface without the exchange of ions or electrons.

In order to explain the adsorption mechanism, FTIR spectroscopy studies were carried out. Adsorption in the IR region takes places due to the rotational and vibrational movements of the molecular groups and chemical bond of a molecule. The two fundamental vibrations are stretching, where the atoms stay in the same bound axis but the distance between atoms increases or decreases, and deformation, where the positions of the atoms change relative to the original bound axis. Fig. 5 represents the FTIR spectra of VT, VTR, and lead adsorbed VTR systems. The broad peak in the region of 3550–3100 cm^{-1} is characteristic of the –OH stretchings of the phenolic and methylol group of tannin. In all spectra, the small peaks in near the 2900 cm^{-1} are due to aromatic C–H stretching vibrations [46,47].

The band at 1732 cm^{-1} in the spectrum of VT belongs to carboxyl–carbonyl groups. The absorption bands between 1604 and 1444 cm^{-1} are related to aromatic –C=C– bonds. The peaks at 1315 and 1037 cm^{-1} in the spectrum of tannin belong to phenol groups [48,49]. The peak at 1160 cm^{-1} is due to aromatic C–H deformation [46]. The deformation vibrations of the C–H bond in the benzene rings also give small absorption bands in the 910–740 cm^{-1} range.

When the spectra of VTR were compared with the IR spectrum of the VT, the peaks at 1732 and 1604 cm^{-1} belonging to C=O and –C=C– are combined and broadened. This broad peak is located at 1671 cm^{-1} with a shoulder at 1604 cm^{-1} which may be attributed to the –C=C– stretching vibration. This change occurs most probably due to environmental change of C=O groups of VTR. Since the formation of methylene bridge in ortho position of C=O groups of VT during the polymerization process will affect the vibration of C=O group. The band intensities between 1732 and 1037 cm^{-1} are reduced and 1732 cm^{-1} peak slightly shifted to 1676 cm^{-1} in the spectrum of the VTR. This situation may be attributed to the –CO stretching of ben-

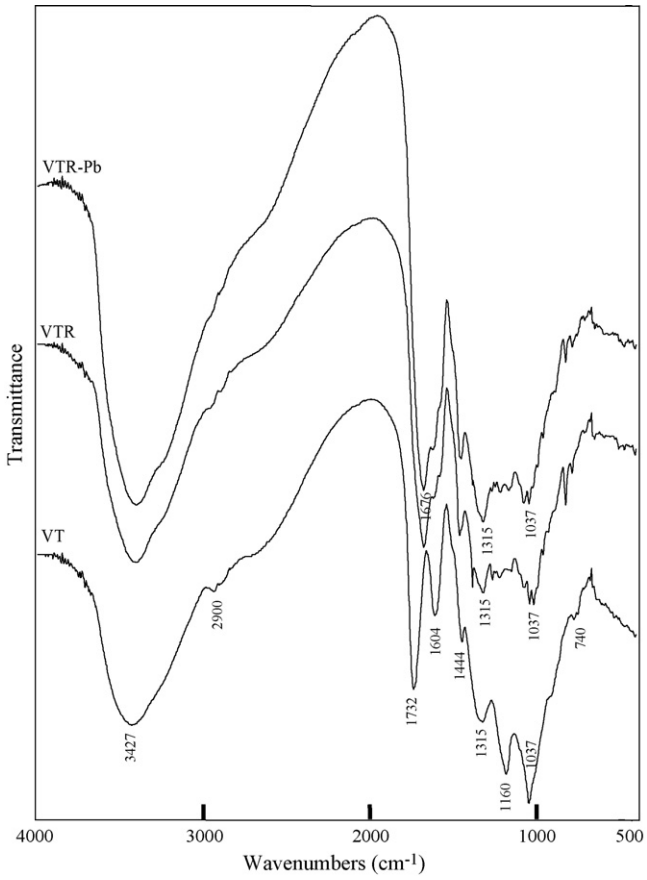

Fig. 5. FTIR spectra of lead-ions adsorbed onto VTR. VT: valonia tannin; VTR: valonia tannin–formaldehyde resin; VTR-Pb: Pb^{2+} adsorbed valonia tannin–formaldehyde resin.

zene ring and the phenolic –OH groups. Also, the formation of $–CH_2–O–CH_2–$ linkage is appeared at 1150–1085 cm^{-1} [47]. The intensity of peak at about 1444 cm^{-1} is slightly increased due to the formation of methylene bridges by reaction with the formaldehyde [48,49].

When the spectra of lead adsorbed VTR were compared with VTR, the relative peak intensities of peak series at 1315 and 1037 cm^{-1} region were changed because of metal–tannate complex formation between lead-ions and some phenolic groups of tannin [50–53].

It is expected that the change in the wide hydroxyl band 3550–3100 cm^{-1} region in the spectra of VTR–lead adsorbed after the ion exchange or complexation reactions between lead-ions and phenolic groups of VTR. But these changes are observed at 1315–1037 cm^{-1} region for the spectra of VTR–lead adsorbed. Because all of the –OH groups in the VTR are not participate in the ion exchange or complexation reactions between the VTR and lead-ions (see Fig. 5). The phenolic groups participating ion exchange or complexation reactions are located in the 1315–1037 cm^{-1} region for VTR. The wide bands in the 3550–3100 cm^{-1} region are belonging to free hydroxyl groups (not participate reactions with lead-ions) of the VTR.

In order to understand the role of the ion exchange proposed for the adsorption mechanism, the effect of pH on the VTR–lead

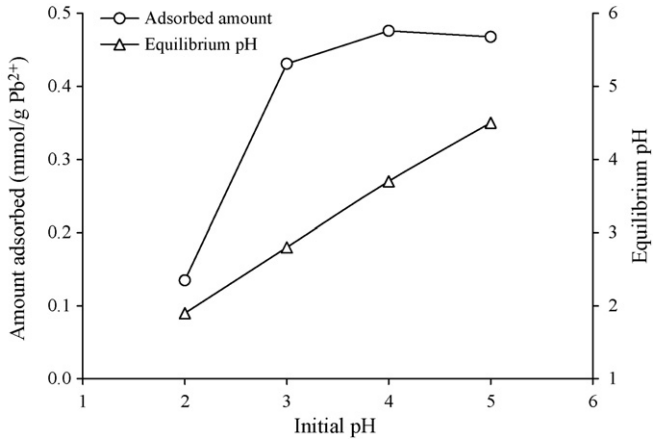

Fig. 6. Effect of pH on adsorption of lead by VTR. Conditions: 75–100 μm particle size, 0.1 g/100 mL dose, 0.483 mmol/L concentration and 298 K temperature.

adsorption system was investigated. The results are shown in Fig. 6. The uptake of lead was strongly affected by solution pH. At initial lead concentration of 0.483 mmol/L, lead adsorption was 0.135 mmol/g at initial solution pH of 2.0, but it increased sharply when initial solution pH rose from 2 to 4 (Fig. 6). Further experiments at initial solution pH above 5 were not conducted due to the precipitation of lead occurring in the solution. Zhan and Zhao [11] stated that lead removal through precipitation took place at pH about 5.

To interpret the adsorption behavior of Pb(II) ions on an adsorbent surface, a knowledge of Pb(II) speciation and the adsorbent surface characteristics is essential [54]. The VTR has multiple adjacent polyhydroxyphenyl groups in its chemical structure which have extremely high affinity for heavy metal ions [3,9,55]. Based on the electron donating nature of the O-containing phenol groups in VTR and the electron-accepting nature of heavy metal ions, the ion exchange mechanism could be preferentially considered. For instance, a divalent heavy metal ion such as Pb^{2+} may attach itself to two adjacent hydroxyl groups which can donate two pare of electrons to the metal ion, forming four coordination number compounds and releasing two hydrogen ions into solution. It is then readily understood that the equilibrium is quite dependent on pH of the aqueous solution. At lower pH, the H^+ ions compete with Pb^{2+} cations for the exchange sites on the VTR, thereby partially releasing the latter. The Pb^{2+} cations are completely released under circumstances of extreme acidic conditions. In most cases, the adsorbed amount of metal ions increased with an increase in pH up to a certain value and then decreased with further increase of pH. In a certain pH range for Pb^{2+}, there may be number of species present in solution, such as Pb^{2+}, $Pb(OH)^+$, $Pb(OH)_2$, etc. At lower pH, the positive charged lead-ion species may compete with H^+ and be adsorbed at the surface of the VTR by ion exchange mechanism. An increase in pH shows an increase in adsorption up to 5 in which the surface of VTR is negatively charged and the adsorbate species are also still positively charged. The increasing electrostatic attraction between positively charged adsorbate species [Pb^{2+} and $Pb(OH)^+$] and negative surface sites will lead to increased adsorption of Pb(II) on VTR. This same pH

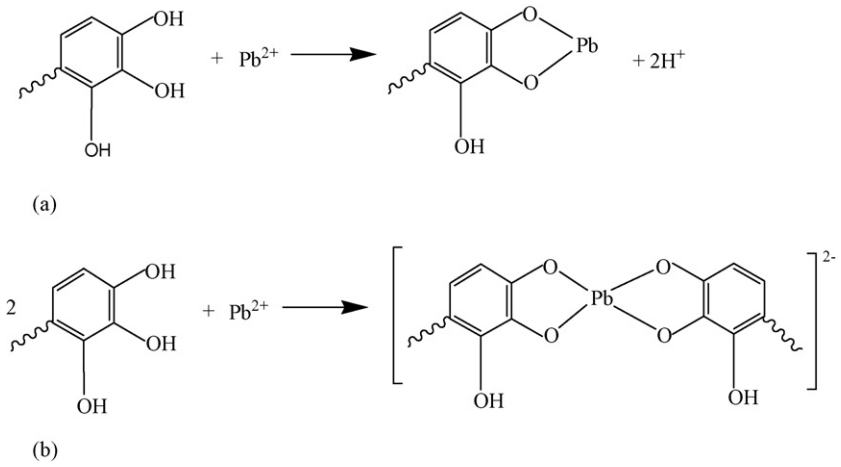

Fig. 7. Adsorption mechanisms for the adsorption of lead-ion onto VTR: (a) ion exchange mechanism between Pb^{2+} and pyrogallol group in VTR surface and (b) complexation mechanism between Pb^{2+} and pyrogallol group in VTR surface.

phenomenon was observed by earlier workers when examining metal adsorption on activated carbon [54].

As can be seen from Fig. 6, the equilibrium pH values were lower than the initial pH values in the solution. It may be inferred that two H^+ ions present on the VTR may be exchanged by one Pb^{2+} ion. Hence, it can be reasonably assumed that ionic exchange may occur in the current adsorption process.

We concluded that the adsorption mechanism may be partly a result of the ion exchange or complexation between the lead-ions and phenolic groups on the VTR surface. Thus, the Pb^{2+}/VTR reaction may be represented in two ways as shown in Fig. 7. Similar reaction pathways are proposed as the adsorption mechanisms for the adsorption of various metal ions onto tannin based adsorbents [10,11,13,39,42,56–58].

4. Conclusion

The results of present investigation show that VTR has considerable potential for the removal of lead from aqueous solution over a wide range of concentration. The adsorbed amounts of lead increased with increase in contact time and reached the equilibrium after 90 min. The equilibrium time is independent of initial lead concentration.

Equilibrium and kinetic studies were conducted for the adsorption of lead from aqueous solutions onto VTR in the concentration range 0.242–1.450 mmol/L at pH 4 and 298 K. The equilibrium data have been analyzed using Langmuir, Freundlich, Temkin and Dubinin–Radushkevich isotherms. The characteristic parameters for each isotherm and related correlation coefficients have been determined. The Langmuir isotherm was demonstrated to provide the best correlation for the adsorption of lead onto VTR. Assuming the batch adsorption to be a single-staged equilibrium operation, the separation process can be defined mathematically using these isotherm constants to estimate the residual concentration of lead or amount of adsorbent for desired purification.

The kinetics of adsorption of lead onto VTR was studied by using pseudo first- and second-order equations, the Elovich equation and intraparticle diffusion equation. All findings presented in this study suggest that lead-VTR system can not be described by the pseudo first-order equation, the Elovich equation and intraparticle diffusion equation. Since the correlation coefficients obtained for these equations are lower than those of pseudo second-order equation, and predicted q_t values considerably deviate from the experimental data points.

For lead-VTR system examined, the pseudo second-order equation provided the best correlation of the experimental data. The pseudo second-order equation is based on the adsorption capacity on the solid phase and is in agreement with a chemisorption mechanism being the rate controlling step. The reaction mechanism may be partly a result of the ion exchange or complexation between the lead-ions and the phenolic groups on the VTR surface.

References

[1] V.J.P. Vilar, C.M.S. Botelho, R.A.R. Boaventura, Influence of pH, ionic strength and temperature on lead biosorption by *Gelidium* and agar extraction algal waste, Process Biochem. 40 (2005) 3267–3275.
[2] H. Ucun, Y.K. Bayhan, Y. Kaya, O.F. Algur, Biosorption of lead(II) from aqueous solution by cone biomass of *Pinus sylvestris*, Desalination 154 (2003) 233–238.
[3] A. Shukla, Y.H. Zhang, P. Dubey, J.L. Margrave, S.S. Shukla, The role of sawdust in the removal of unwanted materials from water, J. Hazard. Mater. 95 (2002) 137–152.
[4] N. Bektaş, B.A. Ağım, S. Kara, Kinetic and equilibrium studies in removing lead ions from aqueous solutions by natural sepiolite, J. Hazard. Mater. B 112 (2004) 115–122.
[5] M. Mouflih, A. Alkik, S. Sebti, Removal of lead from aqueous solutions by activated phosphate, J. Hazard. Mater. B 119 (2005) 183–188.
[6] L. Qi, Z. Xu, Lead sorption from aqueous solutions on chitosan nanoparticles, Colloids Surf. A: Physicachem. Eng. Aspects 251 (2004) 183–190.
[7] Q.Y. Sun, P. Yu, L.Z. Yang, The adsorption of lead and copper from aqueous solution on modified peat-resin particles, Environ. Geochem. Health 26 (2004) 311–317.
[8] Y.S. Ho, J.C.Y. Ng, G. McKay, Removal of lead(II) from effluents by sorption on peat using second-order kinetics, Sep. Sci. Technol. 36 (2001) 241–261.
[9] B. Yu, Y. Zhang, A. Shukla, S.S. Shukla, K.L. Dorris, The removal of heavy metals from aqueous solutions by sawdust adsorption–removal of lead and

comparison of its adsorption with copper, J. Hazard. Mater. B 84 (2001) 83–94.
[10] H. Türkmenler, M. Özacar, İ.A. Şengil, Biosorption of lead onto mimosa tannin resin: equilibrium and kinetic studies, Int. J. Environ. Pollut. 33 (2008) 212–225.
[11] X.-M. Zhan, X. Zhao, Mechanism of lead adsorption from aqueous solutions using an adsorbent synthesized from natural condensed tannin, Water Res. 37 (2003) 3905–3912.
[12] X. Liao, Z. Lu, M. Zhang, X. Liu, B. Shi, Adsorption of Cu(II) from aqueous solutions by tannin immobilized on collagen, J. Chem. Technol. Biotechnol. 79 (2004) 335–342.
[13] A. Nakajima, Electron spin resonance study on the vanadium adsorption by persimmon tannin gel, Talanta 57 (2002) 537–544.
[14] Y. Nakano, M. Tanaka, Y. Nakamura, M. Konno, Removal and recovery system of hexavalent chromium from waste water by tannin gel particles, J. Chem. Eng. Jpn. 33 (2000) 747–752.
[15] T. Matsumura, S. Usuda, Applicability of insoluble tannin to treatment of waste containing americium, J. Alloys Compd. 271 (1998) 244–247.
[16] T. Sakaguchi, A. Nakajima, Accumulation of uranium by immobilized persimmon tannin, Sep. Sci. Technol. 29 (1994) 205–221.
[17] H. Yamaguchi, R. Higashida, I. Sakata, Adsorption mechanism of heavy-metal ion by microspherical tannin resin, J. Appl. Polym. Sci. 45 (1992) 1463–1472.
[18] M.L. Price, L.G. Butler, Rapid visual estimation and spectrophotometric determination of tannin content of sorghum grain, J. Agric. Food Chem. 25 (1977) 1268–1273.
[19] K.H. Inoue, A.E. Hagerman, Determination of gallotannin with rhodanine, Anal. Biochem. 169 (1988) 363–369.
[20] M. Özacar, İ.A. Şengil, Adsorption of metal complex dyes from aqueous solutions by pine sawdust, Bioresour. Technol. 96 (2005) 791–795.
[21] S.R. Shukla, R.S. Pai, Removal of Pb(II) from solution using cellulose-containing materials, J. Chem. Technol. Biotechnol. 80 (2005) 176–183.
[22] J.S. Allen, Q. Gan, R. Matthews, P.A. Johnson, Comparison of optimised isotherm models for basic dye adsorption by kudzu, Bioresour. Technol. 88 (2003) 143–152.
[23] M. Özacar, Equilibrium and kinetic modelling of adsorption of phosphorus on calcined alunite, Adsorption 9 (2003) 125–132.
[24] A. Selatnia, A. Boukazoula, N. Kechid, M.Z. Bakhti, A. Chergui, Y. Kerchich, Biosorption of lead(II) from aqueous solution by a bacterial dead *Streptomyces rimosus* biomass, Bichem. Eng. J. 19 (2004) 127–135.
[25] S.-H. Lin, R.-S. Juang, Heavy metal removal from water by sorption using surfactant-modified montmorillonite, J. Hazard. Mater. 92 (2002) 315–326.
[26] K.K.H. Choy, G. McKay, J.F. Porter, Sorption of acid dyes from effluents using activated carbon, Resour. Conserv. Recy. 27 (1999) 57–71.
[27] K.G. Bhattacharyya, A. Sharma, Adsorption of Pb(II) from aqueous solution by *Azadirachta indica* (Neem) leaf powder, J. Hazard. Mater. B 113 (2004) 97–109.
[28] M. Özacar, İ.A. Şengil, Adsorption of reactive dyes on calcined alunite from aqueous solutions, J. Hazard. Mater. 98 (2003) 211–224.
[29] M. Özacar, Adsorption of phosphate from aqueous solution onto alunite, Chemosphere 51 (2003) 321–327.
[30] M. Özacar, İ.A. Şengil, Application of kinetic models to the sorption of disperse dyes onto alunite, Colloids Surf. A: Physicachem. Eng. Aspects 242 (2004) 105–113.
[31] M. Özacar, İ.A. Şengil, A kinetic study of metal complex dye sorption onto pine sawdust, Process Biochem. 40 (2005) 565–572.
[32] Y. Önal, C. Akmil-Başar, D. Eren, Ç. Sarıcı-Özdemir, T. Depci, Adsorption kinetics of malachite green onto activated carbon prepared from Tunçbilek lignite, J. Hazard. Mater. B 128 (2006) 150–157.
[33] Y.S. Ho, G. McKay, Sorption of dye from aqueous solution by peat, Chem. Eng. J. 70 (1998) 115–124.
[34] Y.S. Ho, G. McKay, Pseudo-second order model for sorption processes, Process Biochem. 34 (1999) 451–465.
[35] Y. Sağ, Y. Aktay, Kinetic studies on sorption of Cr(VI) and Cu(II) ions by chitin, chitosan and *Rhizopus arrhizus*, Biochem. Eng. J. 12 (2002) 143–153.
[36] C.W. Cheung, J.F. Porter, G. McKay, Sorption kinetics for the removal of copper and zinc from effluents using bone char, Sep. Purif. Technol. 19 (2000) 55–64.
[37] E. Lorenc-Grabowska, G. Gryglewicz, Adsorption of lignite-derived humic acids on coal-based mesoporous activated carbons, J. Colloid Interface Sci. 284 (2005) 416–423.
[38] G. Crini, H.N. Peindy, F. Gimbert, C. Robert, Removal of C.I. Basic Green 4 (Malachite Green) from aqueous solutions by adsorption using cyclodextrin-based adsorbent: kinetic and equilibrium studies, Sep. Purif. Technol. 53 (2007) 97–110.
[39] M. Özacar, C. Soykan, İ.A. Şengil, Studies on synthesis, characterization, and metal adsorption of mimosa and valonia tannin resins, J. Appl. Polym. Sci. 102 (2006) 786–797.
[40] M. Özacar, İ.A. Şengil, Effectiveness of tannins obtained from valonia as a coagulant aid for dewatering of sludge, Water Res. 34 (2000) 1407–1412.
[41] E.D. Bliss, Using tannins to produce leather, in: R.W. Hemingway, J.J. Karchesy (Eds.), Chemistry and Significance of Condensed Tannins, Plenum Press, New York, 1989, pp. 493–502.
[42] G. Vázquez, J. González-Álvarez, S. Freire, M. López-Lorenzo, G. Antorrena, Removal of cadmium and mercury ions from aqueous solution by sorption on treated Pinus pinaster bark: Kinetics and isotherms, Bioresour. Technol. 82 (2002) 247–251.
[43] S. Martinez, I. Štern, Inhibitory mechanism of low-carbon steel corrosion by mimosa tannin in sulphuric acid solution, J. Appl. Electrochem. 31 (2001) 973–978.
[44] L.J. Yu, S.S. Shukla, K.L. Dorris, A. Shukla, J.L. Margrave, Adsorption of chromium from aqueous solutions by maple sawdust, J. Hazard. Mater. B 100 (2003) 53–63.
[45] R.W. Hemingway, Key reaction in developing uses for condensed tannins: an overview, in: R.W. Hemingway, J.J. Karchesy (Eds.), Chemistry and Significance of Condensed Tannins, Plenum Press, New York, 1989, pp. 299–304.
[46] S. Kim, H.J. Kim, Curing behavior and viscoelastic properties of pine and wattle tannin-based adhesives studied by dynamic mechanical thermal analysis and FT-IR–ATR spectroscopy, J. Adhes. Sci. Technol. 17 (2003) 1369–1389.
[47] R.M. Silverstein, F.X. Webster, Spectrometric Identification of Organic Compounds, 6th ed., John Wiley & Sons Inc., New York, 1998, pp. 90–91.
[48] J.M. Garro-Galvez, M. Fechtal, B. Riedl, Gallic acid as a model of tannins in condensation with formaldehyde, Thermochim. Acta 274 (1996) 149–163.
[49] T. Holopainen, L. Alvila, J. Rainio, T.T. Pakkanen, IR spectroscopy as a quantitative and predictive analysis meyhod of phenol–formaldehyde resol resins, J. Appl. Polym. Sci. 69 (1998) 2175–2185.
[50] M. Özacar, İ.A. Şengil, Enhancing phosphate removal from wastewater by using polyelectrolytes and clay injection, J. Hazard. Mater. B 100 (2003) 131–146.
[51] M. Özacar, İ.A. Şengil, Effect of tannins on phosphate removal using alum, Turk. J. Eng. Environ. Sci. 27 (2003) 227–236.
[52] J. Araña, E.T. Rendón, J.M. Doña Rodríguez, J.A. Herrera Melián, O. González Díaz, J. Pérez Peña, Highly concentrated phenolic wastewater treatment by the Photo-Fenton reaction, mechanism study by FTIR–ATR, Chemosphere 44 (2001) 1017–1023.
[53] L.M. Zhang, D.Y. Yin, Novel modified lignosulfonate as drilling mud thinner without environmental concerns, J. Appl. Polym. Sci. 74 (1999) 1662–1668.
[54] K.A. Krishnan, A. Sheela, T.S. Anirudhan, Kinetic and equilibrium modeling of liquid-phase adsorption of lead and lead chelates on activated carbons, J. Chem. Technol. Biotechnol. 78 (2003) 642–653.
[55] M. Özacar, İ.A. Şengil, Evaluation of tannin biopolymer as a coagulant aid for coagulation of colloidal particles, Colloids Surf. A: Physicachem. Eng. Aspects 229 (2003) 85–96.
[56] Y. Nakano, K. Takeshita, T. Tsutsumi, Adsorption mechanism of hexavalent chromium by redox within condensed-tannin gel, Water Res. 35 (2001) 496–500.
[57] A. Nakaima, Y. Baba, Mechanism of hexavalent chromium adsorption by persimmon tannin gel, Water Res. 38 (2004) 2859–2864.
[58] Y.H. Kim, Y. Nakano, Adsorption mechanism of palladium by redox within condensed-tannin gel, Water Res. 39 (2005) 1324–1330.

[59] X.M. Zhan, X. Zhao, M. Akane, N. Yoshiho, Removal of lead from aqueous solutions by condensed tannin gel adsorbent, J. Environ. Sci. 15 (2003) 102–106.
[60] J.Y.C. Ng, W.H. Cheung, G. McKay, Equilibrium studies for the sorption of lead from effluents using chitosan, Chemosphere 52 (2003) 1021–1030.
[61] K.K. Wong, C.K. Lee, K.S. Low, M.J. Haron, Removal of Cu and Pb by tartaric acid modified rise husk from aqueous solutions, Chemosphere 50 (2003) 23–28.
[62] B. Chen, C.M. Hui, G. McKay, Film-pore diffusion modeling for the sorption of metal ions from aqueous effluents onto peat, Water Res. 35 (2001) 3345–3356.
[63] R. Shawabkeh, A. Al-Harahsheh, M. Hami, A. Khlaifat, Conversion of oil shale ash into zeolite for cadmium and lead removal from wastewater, Fuel 83 (2004) 981–985.
[64] O. Genç, L. Soysal, G.B. Lu, M.Y. Arica, S. Bektas, Procion green H-4G immobilized poly(hydroxyethyl-methacrylate/chitosan) composite membranes for heavy metal removal, J. Hazard. Mater. 97 (2003) 111–125.
[65] Y. Göksungur, S. Uren, U. Güvenç, Biosorption of cadmium and lead ions by ethanol treated waste baker's yeast biomass, Bioresour. Technol. 96 (2005) 103–109.
[66] J. Rivera-Utrilla, I. Bautista-Toledo, M.A. Ferro-García, C. Moreno-Castilla, Activated carbon surface modifications by adsorption of bacteria and their effect on aqueous lead adsorption, J. Chem. Technol. Biotechnol. 76 (2001) 1209–1215.
[67] G. Yan, T. Viraraghavan, Heavy metal removal from aqueous solution by fungus *Mucor rouxii*, Water Res. 37 (2003) 4486–4496.
[68] Z. Wu, Z. Gu, X. Wang, L. Evans, H. Guo, Effects of organic acids on adsorption of lead onto montmorillonite, goethite and humic acid, Environ. Pollut. 121 (2003) 469–475.
[69] Y.-H. Li, S. Wang, J. Wei, X. Zhang, C. Xu, Z. Luan, D. Wu, B. Wei, Lead adsorption on carbon nanotubes, Chem. Phys. Lett. 357 (2002) 263–266.
[70] S.S. Ahluwalia, D. Goyal, Removal of heavy metals by waste tea leaves from aqueous solution, Eng. Life Sci. 5 (2005) 158–162.